THE JOURNAL OF PHYSICAL CHEMISTRY B

ARTICLE

pubs.acs.org/JPCB

Electrochemistry of Hg(II) Salts in Room-Temperature Ionic Liquids

Ninie S. A. Manan,[†,‡] Leigh Aldous,[†,§] Yatimah Alias,[‡] Richard G. Compton,[§] M. Cristina Lagunas,[*,†] and Christopher Hardacre[*,†]

[†]School of Chemistry and Chemical Engineering, The QUILL Centre, Queen's University, Belfast BT9 5AG, U.K.

[‡]Chemistry Department, Faculty of Science, University of Malaya, 50603, Kuala Lumpur, Malaysia

[§]Department of Chemistry, Physical and Theoretical Chemistry Laboratory, University of Oxford, Oxford OX1 3QZ, U.K.

Supporting Information

ABSTRACT: The electrochemistry of $HgCl_2$ and $[Hg(NTf_2)_2]$ ($[NTf_2]^-$ = bis{(trifluoromethyl)sulfonyl}imide) has been studied in room temperature ionic liquids. It has been found that the cyclic voltammetry of Hg(II) is strongly dependent on a number of factors (e.g., concentration, anions present in the mixture, and nature of the working electrode) and differs from that found in other media. Depending on conditions, the cyclic voltammetry of Hg(II) can give rise to one, two, or four reduction peaks, whereas the reverse oxidative scans show two to four peaks. Diffuse reflectance UV−vis spectroscopy and X-ray powder diffraction have been used to aid the assignment of the voltammetric waves.

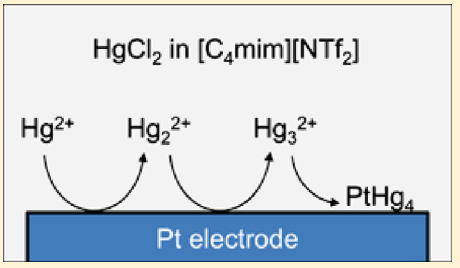

INTRODUCTION

Mercury is a neurotoxic metal which causes damage to the environment and to health, making it a high priority in environmental legislation. Mercury enters the environment through a variety of sources, both natural (e.g., volcanoes) and related to human activity (e.g., emissions from fossil fuel combustion, mining, or solid waste combustion), and it can be found in different chemical forms (e.g., elemental mercury, Hg(II) salts, organomercurials). There is, therefore, increasing demand not only for the reduction of mercury released into the environment but also for better detection and removal methods.

Ionic liquids (ILs) have recently been investigated as a means of sequestering mercury from both liquid and gas streams.[1] However, the speciation of the mercury in the ionic liquids is largely unknown. Ionic liquids are essentially molten salts that are liquid at or near room temperature; among their many useful properties are their high inherent conductivity, wide electrochemical stability, negligible volatility, tunable miscibility, and unique solvating characteristics.[2] These properties make the ILs an alternative media for the remediation of mercury. The low vapor pressure prevents significant vaporization of the ionic liquid and with it the mercury and the tenability allows efficient design of sequestering moieties to be added to the cation/anion. Recovery of the ionic liquid is vital due to their cost and, therefore, due to the high conductivity of the media, electrochemistry presents an attractive method of IL remediation once they have become saturated with Hg. Furthermore, Hg is an attractive electrode material for fundamental electrochemical studies. However, before such goals can be adequately realized, fundamental studies into the electrochemical behavior of Hg in ILs are required.

Studies on the electrochemistry of mercury in room temperature ILs are very limited, with only one work published, to date, and which focuses in the water- and air-sensitive $AlCl_3$−$[C_2mim]Cl$ ($[C_2mim]^+$ = 1-ethyl-3-methylimidazolium).[3] Therein, in acidic $AlCl_3$−$[C_2mim]Cl$ (66.7−33.3 mol %) mixtures, cyclic voltammetry at glassy carbon or tungsten working electrodes shows that $HgCl_2$ is reduced in two steps to Hg_2^{2+} and mercury metal (eqs 1 and 2). However, in basic 44.4−55.6 mol % $AlCl_3$−$[C_2mim]Cl$, a chloride Hg(II) complex forms which is then reduced in a single step to Hg(0) (eq 3). It was also found that Hg_2Cl_2 rapidly disproportionates in the Lewis basic mixture (eq 4). Both in acidic and basic mixtures, a single oxidative stripping peak is observed in the reverse scans. Related studies on molten salts at high temperature showed analogous results. Thus, $HgCl_2$ shows one single reduction from Hg(II) to Hg(0) at Pt working electrodes in molten LiCl−KCl (450 °C)[4,5] or $ZnCl_2$−KCl (300 °C),[6] with Hg(I) species not observed in these systems. It should be noted that at high scan rates, i.e., between 3.7 and 45.8 V s^{-1}, the cyclic voltammetry of $HgCl_2$ in $ZnCl_2$−KCl contains a prewave preceding the bulk reduction of Hg(II) to Hg(0) which is related to the adsorption of mercury. Accordingly, the reverse scans also show two oxidation peaks.[6] In addition, it has also been shown that the Hg(II)/Hg(0) reduction is reversible at high scan rates, but at low scan rates the metal deposits onto the electrode and reacts to form $PtHg_4$.[5,6]

$$2Hg^{2+} + 2e^- \rightarrow Hg_2^{2+} \quad (1)$$

$$Hg_2^{2+} + 2e^- \rightarrow 2Hg \quad (2)$$

$$[HgCl_{2+x}]^{x-} + 2e^- \rightarrow Hg + (2+x)Cl^- \quad (3)$$

$$Hg_2Cl_2 + xCl^- \rightarrow [HgCl_{2+x}]^{x-} + Hg \quad (4)$$

Received: December 17, 2010
Revised: January 26, 2011
Published: February 28, 2011

In Lewis acidic chloroaluminate melts, it has been possible to detect stable Hg(I) species.[7,8] For example, Hames and Plambeck[7] reported that the reduction of $HgCl_2$ in $AlCl_3$−NaCl−KCl eutectic at 150 °C at tungsten electrodes occurs in two steps (eqs 1 and 2). These studies also showed that Hg(0) deposited at the electrode reacts with diffusing Hg^{2+} thus decreasing the amount of mercury metal available for electrochemical oxidation. In $AlCl_3$−NaCl melts (175 °C), using a Pt working electrode, Torsi et al.[8] observed three 2-electron-reduction steps for Hg(II): first to Hg_2^{2+} (eq 1), then to Hg_3^{2+} (detected for the first time; eq 5) and finally to Hg(0) (eq 6).

$$3Hg_2^{2+} + 2e^- \rightarrow 2Hg_3^{2+} \quad (5)$$

$$Hg_3^{2+} + 2e^- \rightarrow 3Hg \quad (6)$$

In the present paper, the electrochemistry of $HgCl_2$ has been studied in a series of room temperature ionic liquids. The effect of varying the concentration of the solution, the nature of the working electrode, and the cation/anion of the ionic liquid has been analyzed. Solutions with added chloride at various concentrations have also been studied. For comparison, the cyclic voltammetry of $[Hg(NTf_2)_2]$ has been carried out in $[C_4mim][NTf_2]$. Specific mechanistic insights include the observation that the reduction of Hg^{2+} to Hg(0) takes place in three steps via the formation of intermediate species Hg_2^{2+} and Hg_3^{2+}. In addition, during the reoxidation of Hg four species are observed related to Hg_2^{2+}, Hg^{2+}, and the oxidation of Cl^- bound mercury complexes, including $[HgCl_3]^-$ and $[HgCl_4]^{2-}$, even in mixtures in the absence of added chloride.

EXPERIMENTAL SECTION

The ionic liquids $[C_4mim][NTf_2]$ ($[C_4mim]^+$ = 1-butyl-3-methylimidazolium),[9] $[C_4mim]Cl$,[10] and $[C_4mim][NO_3]$[11] were prepared following published procedures. The ionic liquids $[C_nmim][NTf_2]$ ($[C_nmim]^+$ = 1-alkyl-3-methylimidazolium; n = 2, 6, 8), $[C_4py][NTf_2]$ ($[C_4py]^+$ = *N*-butylpyridinium), $[C_4mim][X]$ ($[X]^-$ = DCA (dicyanamide), and FAP (tris(pentafluoroethyl)trifluorophosphate), PF_6) were supplied by Merck KGaA and were purified before use as described elsewhere.[11] The water content of the purified ILs was near or below the level of detection of Karl Fischer titration (<0.01% w/w). Mercury(II) chloride (Aldrich) was used as received and handled in a glovebox.

$[Hg(NTf_2)_2]$[12] was prepared by mixing a solution of $H[NTf_2]$ (1.29 g, 4.6 mmol) in 1 cm^3 of H_2O with an aqueous solution of HgO (0.5 g, 2.3 mmol). The mixture was stirred for 10 min at room temperature resulting in the precipitation of a yellow powder. The water layer was decanted and the yellow powder was washed with diethyl ether several times. The remaining solvent was removed in a rotary evaporator and the yellow solid further dried under vacuum at 60 °C (0.92 g, 51%). The elemental analysis suggests that the $[Hg(NTf_2)_2]$ obtained still contains some water (found: C, 6.23; H, 0.59; N, 3.27; S, 16.24%. $C_4N_2F_{12}HgO_8S_4 \cdot H_2O$ requires C, 6.17; H, 0.26; N, 3.60; S, 16.43%)

Solutions of $HgCl_2$ or $[Hg(NTf_2)_2]$ in the ionic liquids were prepared by adding the mercury compound to 2 cm^3 of the corresponding IL in a glovebox and leaving the mixture to stir for 24 h before analysis. Saturated solutions $HgCl_2$ in $[C_4mim][NTf_2]$ were prepared in a similar way using an excess of $HgCl_2$ (ca. 0.025 g). The concentration of the saturated solution was estimated using a Milestone DMA-80 Direct Mercury Analyzer wherein 0.01 cm^3 of the saturated solution was diluted by a factor of 100 in ethanol and analyzed. After three readings, the average concentration of the solution was determined to be 28 mM. Solutions of $HgCl_2$ (20 mM) in $[C_4mim][NTf_2]$ in the presence of chloride were prepared in a similar manner as described above by adding $[C_4mim]Cl$ (40 mM, 0.0139 g; 60 mM, 0.0210 g; 80 mM, 0.0279 g) at the same time as $HgCl_2$.

Cyclic voltammograms (CVs), bulk electrolysis, and chronoamperometric experiments were carried out in a PC-controlled AUTOLAB PGSTAT12/30/302 potentiostat/galvanostat using a three-electrode cell. A glassy carbon (GC) disk (diameter 3 mm) or a Pt disk (diameter 1.5 mm) electrode was used as working electrode (WE). Platinum wire was used as the counter electrode. The reference electrode was an Ag/Ag^+ reference electrode containing a Ag wire immersed in a 0.01 M solution of $AgNO_3$ in $[C_4mim][NO_3]$ which was separated from the bulk solution by a glass frit. The glassy carbon WE was polished to a mirror with a water-based diamond slurry and rinsed with ultrapure water before use, and the Pt WE was polished with aluminum oxide (3 μm particle size). For the bulk electrolysis experiment, Pt foil (0.5 × 0.7 cm) was used as WE while the counter and reference electrodes were the same as described above. All the electrochemical measurements were performed in a glovebox.

The diffusion coefficient of $[HgCl_{2+x}]^{x-}$ in $[C_4mim][NTf_2]$ (i.e., from solutions of $HgCl_2$ in $[C_4mim][NTf_2]$ with excess Cl^-) was estimated from cyclic voltammetric data at various scan rates using the Randles−Sevcik equation adapted to irreversible systems (i.e., from the plot of peak current vs square root of scan rate). The number of electrons transferred and the αn product (α = electron transfer coefficient) were calculated using a Tafel plot. For comparison, the value of the diffusion coefficient was also calculated from chronoamperometric data using the Cottrell equation.

Diffuse reflectance (DR) UV−vis spectra were recorded on a Perkin-Elmer, Lambda 650 S UV/vis spectrometer with an integrating sphere detector. A drop of $[C_4mim][NTf_2]$ was spread on the surface of a Teflon holder and used as blank. Similarly, a drop of each sample solution was spread on the surface of the Teflon holder and the spectrum recorded from 800 to 200 nm. X-ray powder diffraction was performed on the Pt or GC electrodes after electrolysis using a X'Pert Pro PANalytical diffractometer with Cu Kα radiation (λ = 1.5418 Å). The patterns obtained were compared against literature data.

RESULTS AND DISCUSSION

A summary of the proposed reactions and peak assignments for the CVs of Hg(II) in ILs is shown in Table 1.

Electrochemistry of $[Hg(NTf_2)_2]$ in $[C_4mim][NTf_2]$. The cyclic voltammetry of a ca. 20 mM solution of $[Hg(NTf_2)_2]$ was performed in $[C_4mim][NTf_2]$ at GC and Pt electrodes (Figure 1). In both cases, one broad reduction peak was observed [R_1 = −0.03 V (GC), 0.11 V (Pt)], with a symmetrical stripping wave appearing in the reverse scans [O_{1a} = 0.83 V (GC), 0.72 V (Pt)]. These peaks are assigned to the two-electron reduction of Hg(II), presumably in the form of a bis{(trifluoromethyl)sulfonyl}imide-containing species, to Hg(0), as shown in eq 7a, and the corresponding inverse oxidation reaction.

$$[Hg^{2+}]_{NTf2} + 2e^- \rightarrow Hg \quad (7a)$$

Electrochemistry of $HgCl_2$ at GC Electrode. *Electrochemistry of $HgCl_2$ in $[C_4mim][NTf_2]$.* The cyclic voltammetries of a 5 mM and a saturated solution of $HgCl_2$ in $[C_4mim][NTf_2]$ were

dx.doi.org/10.1021/jp1120096 |*J. Phys. Chem. B* 2011, 115, 2574–2581

Table 1. Summary of the Proposed Reactions and Peak Assignments

peak		reaction	
R_1		$[Hg^{2+}]_{NTf2} + 2e^- \rightarrow Hg$	(7a)
	or	$[Hg^{2+}]_{NTf2/Cl} + 2e^- \rightarrow Hg$	(7b)
R_2		$[Hg^{2+}]_{Cl} + 2e^- \rightarrow 2Hg^-$	(8)
R_{2a}		$2Hg^{2+} + 2e^- \rightarrow Hg_2^{2+}$	(1)
R_{2b}		$3Hg_2^{2+} + 2e^- \rightarrow 2Hg_3^{2+}$	(5)
R_{2c}		$Hg_3^{2+} + 2e^- \rightarrow 3Hg$	(6)
R_3		$[HgCl_{2+x}]^{x-} + 2e^- \rightarrow Hg + (2+x)Cl^-$	(3)
R_4		$Cl_2 + 2e^- \rightarrow 2Cl^-$	(13')
O_{1a}		$Hg \rightarrow [Hg^{2+}]_{NTf2} + 2e^-$	(7a')
O_1		$2Hg + 2Cl^- \rightarrow Hg_2Cl_2(s) + 2e^-$	(10)
	and/or		
	followed by	$Hg \rightarrow Hg^{2+} + 2e^-$	(11)
		$Hg + Hg^{2+} + 2Cl^- \rightarrow Hg_2Cl_2(s)$	(9)
O_2		$Hg_2Cl_2(s) \rightarrow 2Hg^{2+} + 2Cl^- + 2e^-$	(12)
O_3/O_{3a}		$2[Cl^-]_{Hg(II)} \rightarrow Cl_2 + 2e^-$	(14)
O_4		$2Cl^- \rightarrow Cl_2 + 2e^-$	(13)
O_5		$Hg + (2+x)Cl^- \rightarrow [HgCl_{2+x}]^{x-} + 2e^-$	(3')

studied at GC. The concentration of the saturated solution was estimated to be 28 mM (see Experimental Section). The 5 mM solution showed two reduction peaks, i.e., a small peak at −0.27 V (R_1) and a larger peak at −0.64 V (R_2). The reverse scan displayed three oxidation peaks at −0.35 V (O_1), −0.04 V (O_2), and 1.49 V (O_{3a}) (Figure 2a, solid line). Peaks R_2 and O_2 have the characteristic sharp shape of a deposition and stripping process, respectively. When the sweep is reversed after R_1 (Figure 2a, dashed line) the anodic scan shows initially some cathodic current but no clear oxidation peaks. Analogous results were obtained from a saturated solution (Figure 2b, solid line); however, in this case, the two reduction peaks R_1 (−0.35 V) and R_2 (−0.72 V) are of similar intensity. In addition, the third oxidation peak appears split, with a maximum at 1.54 V (O_3) and a shoulder at ca. 1.42 V (O_{3a}).

The first reduction peak is slightly shifted with respect to that observed in the $[Hg(NTf_2)_2]$ solution at GC (Figure 1); but a good match between the first reduction peak of $[Hg(NTf_2)_2]$ and $HgCl_2$ in $[C_4mim][NTf_2]$ is found at Pt electrodes (see below). It is, therefore, suggested that a small amount of a Hg(II) bis{(trifluoromethyl)sulfonyl}imide complex and/or a mixed $[NTf_2]^-/Cl^-$ species forms in the $HgCl_2/[C_4mim][NTf_2]$ mixtures which is reduced to Hg(0) (eqs 7a and 7b, Table 1) at a more positive potential than the main Hg(II) species present in the $HgCl_2$ solution, $[Hg^{2+}]_{Cl}$. The second reduction peak, R_2, is assigned to the reduction of $[Hg^{2+}]_{Cl}$ to Hg(0) (eq 8).

$$[Hg^{2+}]_{Cl} + 2e^- \rightarrow 2Hg \quad (8)$$

Bulk electrolysis was carried out at the two reduction peaks for the saturated solution at GC plates. In both cases, a white paste was observed at the GC surface. The deposits were analyzed using X-ray powder diffraction (see Supporting Information) and showed

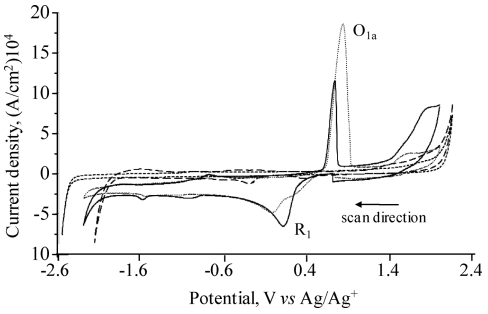

Figure 1. Cyclic voltammograms of a 20 mM solution of $[Hg(NTf_2)_2]$ in $[C_4mim][NTf_2]$ at GC (small dot line) or Pt (solid line) electrode. Also included are background scans of $[C_4mim][NTf_2]$ at GC (dotted line) and Pt (dashed line). Scan rate 100 mV s^{-1}.

similar patterns which corresponded well to that of Hg_2Cl_2.[13] The formation of Hg_2Cl_2 during bulk electrolysis is mainly attributed to the reaction of electrogenerated Hg(0) with excess Hg^{2+}, as shown in eq 9.[14] In addition, direct reduction of Hg^{2+} to $Hg_2Cl_2(s)$ may occur to some extent at R_1 during the cyclic voltammetry.

$$Hg + Hg^{2+} + 2Cl^- \rightarrow Hg_2Cl_2(s) \quad (9)$$

The presence of a cathodic current in the anodic scans when the sweep is reversed after R_1 (Figure 2, a and b, dashed lines) indicates nucleation of Hg at the electrode surface. The small shift observed in R_2 when the scan is first run toward positive potential (Figure 1b, dotted line) may be attributed to passivation of the electrode surface, for example, by chlorine formed at high potential from traces of chloride present as an impurity in the ionic liquid.[15,16]

The occurrence of several oxidation peaks in the reverse scans (Figure 2) contrasts with that observed in $[Hg(NTf_2)_2]/[C_4mim][NTf_2]$ solutions (Figure 1) and for $HgCl_2$ in $AlCl_3-[C_2mim]Cl$,[3] where only one stripping peak is found. A comparison between Figures 1 and 2 indicates that none of the peaks O_1-O_3 correspond to the formation of a Hg(II) bis{(trifluoromethyl)sulfonyl}imide species. In addition, there is no evidence of free chloride remaining in the solution after O_1 (i.e., the oxidation of free Cl^- to Cl_2 at GC in $[C_4mim][NTf_2]$ should appear as a peak at 1.1 V;[17] see below). Taking the above into account, the first oxidation wave, O_1, may be assigned to the formation of Hg_2^{2+}, probably as $Hg_2Cl_2(s)$, at the electrode surface, either by direct oxidation of Hg to $Hg_2Cl_2(s)$ (eq 10) and/or by oxidation to Hg^{2+} (eq 11) followed by reaction 9. The second oxidation peak, O_2, would then correspond to the stripping of $Hg_2Cl_2(s)$ to form Hg^{2+} (eq 12). Finally, the peaks at ca. 1.5 V (O_3 and O_{3a}) are initially attributed to the oxidation of mercury chloride species formed during the electrochemical cycle. This is discussed further in the next section.

$$2Hg + 2Cl^- \rightarrow Hg_2Cl_2(s) + 2e^- \quad (10)$$

$$Hg \rightarrow Hg^{2+} + 2e^- \quad (11)$$

$$Hg_2Cl_2(s) \rightarrow 2Hg^{2+} + 2Cl^- + 2e^- \quad (12)$$

Electrochemistry of $HgCl_2$ in $[C_4mim][NTf_2]$ in the Presence of $[C_4mim]Cl$. In order to provide a more detailed understanding of the electrochemical behavior of $HgCl_2$ in $[C_4mim][NTf_2]$, the effect of adding chloride to a 20 mM solution of $HgCl_2$ was analyzed at GC (Figure 3). Chloride was added as $[C_4mim]Cl$ at

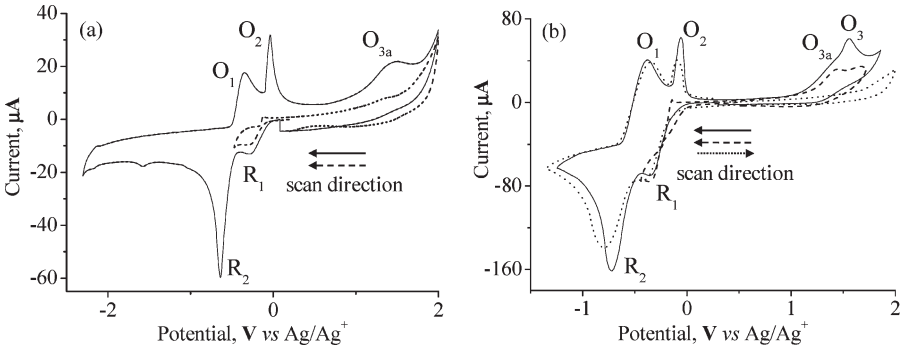

Figure 2. Cyclic voltammograms of a 5 mM (a) and a saturated (b) solution of $HgCl_2$ in $[C_4mim][NTf_2]$ at GC electrode; 100 mV s^{-1}.

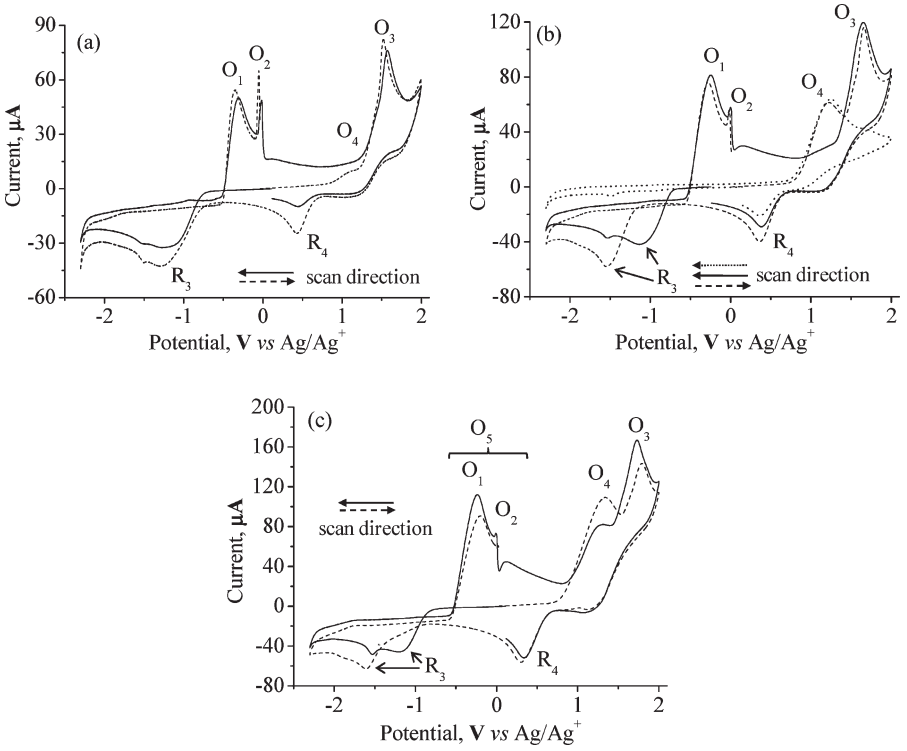

Figure 3. Cyclic voltammetry of a 20 mM solution of $HgCl_2$ in $[C_4mim][NTf_2]$ in the presence of (a) 40 mM, (b) 80 mM, and (c) 120 mM of $[C_4mim]Cl$. Part b also contains the cyclic voltammogram of a 40 mM solution of $[C_4mim]Cl$ in $[C_4mim][NTf_2]$ (dotted line). All scans were run at GC electrode and scan rate of 100 mV s^{-1}.

three different concentrations: 40 mM (Figure 3a), 80 mM (Figure 3b), and 120 mM (Figure 3c). The DR UV−vis spectra of the solutions were also carried out.

In the case of the solution with the least amount of added Cl^- (40 mM, Figure 3a), the scan run first toward positive potential (dashed line) shows an oxidation wave at 1.5 V (O_3) together with a very small peak at 1.1 V (O_4). The latter corresponds to the oxidation of free Cl^- to Cl_2 (eq 13), as previously reported.[17] Its very low intensity indicates that effectively all the added chloride is bound to Hg(II), i.e., probably forming the stable chloromercurate anion $[HgCl_4]^{2-}$. A smaller amount of other species, such as $[HgCl_3]^-$, may also be present in the solution, as indicated by DR UV−vis spectroscopy (see below). As expected, the relative intensity of O_4 increases with added Cl^- (Figure 3b,c, dashed lines).

$$2Cl^- \rightarrow Cl_2 + 2e^- \qquad (13)$$

Peak O_3, which is present in the scans run first toward positive potential for all three solutions (Figure 3, dashed lines), and peak O_{3a} (Figure 2) are, therefore, assigned to the oxidation of Cl^- bound to Hg(II) (eq 14). Given that peaks O_3 and O_{3a} are present in the CVs of $HgCl_2$ without added chloride (Figure 2), chloromercurate(II) anions should form in the proximity of the electrode after reaction 12, from the chemical reaction of Hg^{2+} and excess Cl^-.

$$2[Cl^-]_{Hg(II)} \rightarrow Cl_2 + 2e^- \qquad (14)$$

Generation of Cl_2 at peaks O_3 and O_4 is confirmed by the presence of reduction peak R_4 (0.35 V) in the reverse scans (Figure 3), and which corresponds to the reduction of Cl_2 to Cl^-.[17] For comparison, the cyclic voltammogram of a 40 mM solution of $[C_4mim]Cl$ in $[C_4mim][NTf_2]$ is included in Figure 3b. This further confirms the origin of peaks O_4 and R_4.

dx.doi.org/10.1021/jp1120096 |J. Phys. Chem. B 2011, 115, 2574–2581

From the cyclic voltammograms in Figure 3, it can be seen that the stripping peak O_2 decreases with added chloride, with one very broad wave (O_5) emerging as the concentration of Cl^- increases. In the presence of excess Cl^-, Hg_2Cl_2 is not stable (eq 4), and O_5 is, therefore, assigned to the oxidation of Hg(0) directly to anionic species of the type $[HgCl_{2+x}]^{x-}$ (x = 1 or 2; eq 3′)

$$Hg + (2 + x)Cl^- \rightarrow [HgCl_{2+x}]^{x-} + 2e^- \qquad (3')$$

In the scans run toward negative potential first (Figure 3, solid lines), one broad reduction peak (R_3) at ca. −1.1 V was observed for all three solutions. Peak R_3 is assigned to the reduction of $[HgCl_{2+x}]^{x-}$ to Hg(0) (eq 3) and it appears at more negative potential than peaks R_1 and R_2 in the solutions with no added chloride (Figure 2). This is consistent with the formation of stable chloromercurate(II) species. Analogous behavior has been found in basic chloroaluminate ionic liquids[3] and molten alkali metal chlorides,[4−6] where, in excess Cl^-, Hg(I) species are not detected and stable mercury chloride species are reduced in one 2-electron step to Hg(0) (see eqs 3 and 4).

Reduction peak R_3 also appears when the scans are run first toward positive potential (Figure 3, dashed lines); however, a cathodic shift is observed in Figure 2, b and c. This may be due to passivation of the glassy carbon electrode by electrogenerated chlorine at the upper potential limit.[15,16] For example, it has been shown that chlorine formed at highly positive potentials can attack the glassy carbon surface, rendering it less susceptible to adsorption.[16] This may prevent $[HgCl_{2+x}]^{x-}$ for approaching the electrode surface, thus making more difficult its reduction.

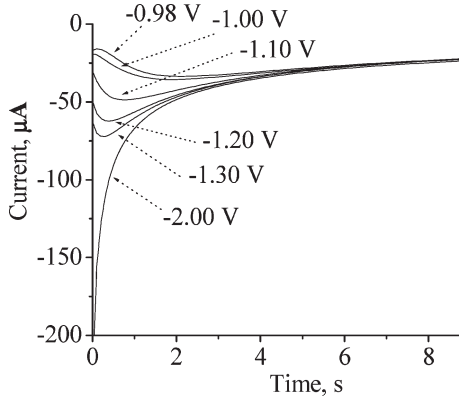

Figure 4. Chronoamperometry at a GC electrode of a solution of $HgCl_2$ (20 mM) and $[C_4mim]Cl$ (40 mM) in $[C_4mim][NTf_2]$ using E_{end} values between −0.98 and −2 V.

All the voltammograms in Figure 3 show current crossover in the scans reversed after R_3, indicating nuclei formation at the electrode surface. The requirement of large nucleation overpotentials for the deposition of Hg from $[HgCl_{2+x}]^{x-}$ solutions parallels that observed in basic $AlCl_3$−$[C_2mim]Cl$ mixtures, where metal deposition was found to occur through instantaneous or progressive nucleation at GC or W electrodes, respectively.[3] Herein, chronoamperometric studies on the $HgCl_2$ solution containing 40 mM of added chloride were carried out to study the nucleation of mercury at the GC electrode. Chronoamperograms were obtained upon stepping the potential from the open-circuit potential (OCP) to potentials (E_{end}) ranging from −0.98 to −2 V. Nucleation peaks were observed only at E_{end} between −0.98 V and −1.3 V (Figure 4; the profiles obtained at −2 V < E_{end} < −1.3 V were similar to that at −2 V and are not included in the figure). Analysis of the nucleation curves according to the Scharifker−Hills model[18] indicated that the process takes place mainly through instantaneous nucleation. However, while very good fittings are obtained for E_{end} = −0.98 or −1 V, increasing deviation from the simulated instantaneous nucleation curve is observed as the end potential becomes more negative. Examples of the dimensionless $(I/I_M)^2$ vs (t/t_M) plots at both extremes are shown in Figure 5 (see Supporting Information for plots at other E_{end} values). Deviations from the theoretical models are not uncommon and are often attributed to a departure from the hemispherical geometry assumed in the nucleation models.[19] Another possibility is that the deviations may reflect the severe approximations made in the analytical theory used.[20]

The effect on the reduction of Hg(II) of varying scan rate was also studied in the case of the $HgCl_2$ solution containing 40 mM of added chloride. The peak currents for R_3 and O_2 increase linearly with the square root of scan rate, indicating that they correspond to diffusion-controlled processes (see Supporting Information). The number of electrons transferred at R_3 was estimated to be 2, in agreement with eq 3. The diffusion coefficient of $[HgCl_{2+x}]^{x-}$ in $[C_4mim][NTf_2]$ was calculated to be 2.5 × 10^{-11} or 2 × 10^{-11} m^2 s^{-1} from cyclic voltammetry or chronoamperometry data, respectively. This is similar to the diffusion coefficient reported for $[HgCl_{2+x}]^{x-}$ in basic $AlCl_3$−$[C_2mim]Cl$ at 40 °C (3 × 10^{-11} m^2 s^{-1}).[3]

Cyclic Voltammetry of $HgCl_2$ at Pt Electrode. *Cyclic Voltammetry of $HgCl_2$ in $[C_4mim][NTf_2]$.* The electrochemistry of a 5 mM and a saturated solution of $HgCl_2$ in $[C_4mim][NTf_2]$ was also investigated using a Pt working electrode. The 5 mM solution showed similar behavior to that observed at GC, with two reduction (R_1 0.07 V, R_2 −0.47 V) and two oxidation peaks

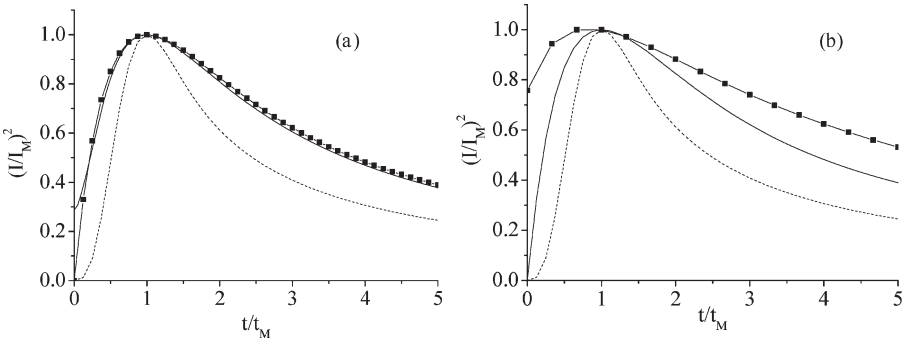

Figure 5. Dimensionless plots generated from the nucleation profiles at E_{end} = −1 V (a) and E_{end} = −1.3 V (b), overlaid with the simulated data for progressive (dashed lines) and instantaneous (solid lines) nucleation processes.

dx.doi.org/10.1021/jp1120096 |J. Phys. Chem. B 2011, 115, 2574–2581

(O_1 −0.37 V, O_2 0.07 V) present in the cyclic voltammogram (see Supporting Information). These four peaks are, therefore, assigned as above (see also Table 1). Both reduction peaks are shifted toward less negative potential with respect to those at GC (−0.27 and −0.64 V), probably as a consequence of the more active Pt electrode surface compared with GC.

Interestingly, in the saturated solution, four reduction peaks at 0.07, −0.26, −0.42, and −0.59 V were found, whereas the two main oxidation peaks (O_1 and O_2) remained largely the same as in the dilute solution. Figure 6 shows the cyclic voltammograms for a saturated solution where scans are reversed after each reduction peak. The second and third reductions both appear to be associated to the stripping peak at −0.04 V (O_2); and the fourth reduction is coupled to the oxidation peak at −0.39 V (O_1). Peaks R_{2a}−R_{2c} are tentatively assigned to the successive reductions of Hg^{2+} to Hg_2^{2+} (eq 1), then to Hg_3^{2+} (eq 5), and finally to Hg(0) (eq 6). This behavior resembles the three-step reduction of Hg reported in $AlCl_3$−NaCl mixtures at Pt electrode.[8] The trinuclear Hg_3^{2+} cation is highly unstable and is expected to form Hg_2Cl_2 when in contact with excess Hg(II) from the solution (eq 15).[8] This would explain the presence of a stripping peak (O_2) when the voltammetric scan is reversed after R_{2a} or R_{2b}.

$$Hg_3^{2+} + Hg^{2+} + 4Cl^- \rightarrow 2Hg_2Cl_2 \qquad (15)$$

Bulk electrolysis was carried out at the four reduction potentials at Pt plates. A white-blue paste was observed on the surface of the Pt plate at the first reduction peak, whereas a gray paste was deposited at the Pt surface for the other three potentials studied. The nature of these initial deposits was not investigated. After a few days in the glovebox, all the deposits dried and became black coatings on the surface of the Pt plates. These black residues were analyzed by XRPD which confirmed that they corresponded to $PtHg_4$ in all cases[21] (see Supporting Information). Formation of $PtHg_4$ when Hg(0) is in contact with a Pt wire for an extended period of time is well-known[22] and has also been reported to form during the reduction of Hg(II) at Pt electrodes in molten salts.[5,6]

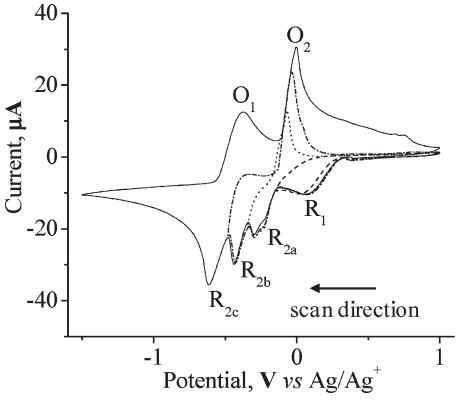

Figure 6. Cyclic voltammograms reversed at different potentials for a saturated solution of $HgCl_2$ in $[C_4mim][NTf_2]$. All scans were run at a Pt electrode and scan rate of 100 mV s^{-1}.

Cyclic Voltammetry of $HgCl_2$ in Other Ionic Liquids at GC and Pt. The cyclic voltammetry of $HgCl_2$ was also examined in other ILs at GC and Pt with both electrodes showing similar behavior (Figure 7 and Supporting Information). The effect of varying the cation was studied using four $[NTf_2]^-$ anion based ionic liquids ($[C_2mim][NTf_2]$, $[C_6mim][NTf_2]$, $[C_8mim][NTf_2]$, and $[C_4py][NTf_2]$). All the $HgCl_2$ solutions (5 mM) showed similar electrochemical behavior as that found in $[C_4mim][NTf_2]$, with two reduction peaks (R_1 and R_2) and three main oxidation peaks (O_1−O_3/O_{3a}) observed in all cases (Figure 7a). The second reduction peak in $[C_8mim][NTf_2]$ appears at −0.93 V and is significantly shifted toward more negative potential compared with the other ionic liquids, where the reduction is seen at ca. −0.6 V. This may be due to the fact that $[C_8mim][NTf_2]$ has the highest viscosity (see Supporting Information for viscosity data) and could also be associated with the formation of solvent multilayers on the electrode surface, presumably related to the long side chain in $[C_8mim][NTf_2]$. The formation of multilayer architectures on electrode surfaces which are dependent on the nature of the IL ions has been suggested to have a strong influence on electrochemical reactions.[23]

The influence of the anion was analyzed in the series $[C_4mim][X]$ (X = DCA, FAP, PF_6). The CV in $[C_4mim][PF_6]$ is similar to that found in $[C_4mim][NTf_2]$ and the peaks are assigned to analogous processes, whereas the voltammetry in $[C_4mim][FAP]$ shows two ill-defined reduction peaks, but no clear oxidation features (see Supporting Information). The different oxidation behavior can be due to different stability of mercury species in the $[FAP]^-$ ionic liquid or to the formation of different solvation layers on the electrode surface,[23] possibly related to the larger size and asymmetry of the $[FAP]^-$ anion, compared with $[PF_6]^-$ and $[NTf_2]^-$. The CV in $[C_4mim][DCA]$ (Figure 7b) resembles that of $[C_4mim][NTf_2]$ with excess Cl^-, with one broad reduction peak observed. The DCA anion behaves as a pseudo-halide ligand and it is, therefore, expected that dicyanamide−Hg(II)

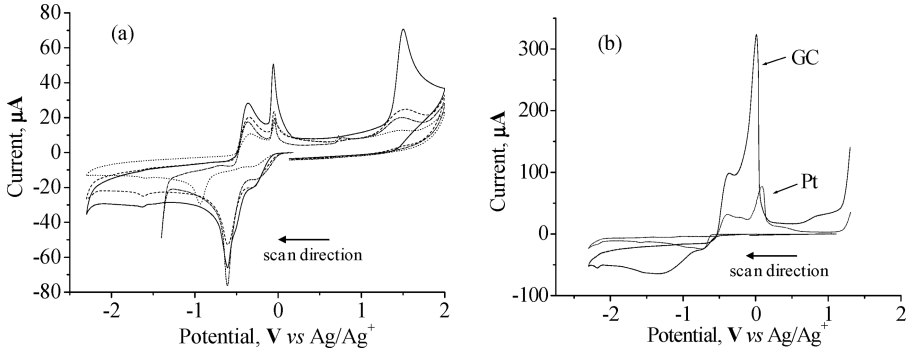

Figure 7. Cyclic voltammograms of 5 mM solutions of $HgCl_2$ in (a) $[C_2mim][NTf_2]$ (solid line), $[C_6mim][NTf_2]$ (dashed line), $[C_8mim][NTf_2]$ (dotted line) and $[C_4py][NTf_2]$ (dash-dot) at GC electrode; and (b) in $[C_4mim][DCA]$ at GC (solid line) and Pt (dotted line) electrodes. Scan rate: 100 mV s^{-1}.

dx.doi.org/10.1021/jp1120096 |J. Phys. Chem. B 2011, 115, 2574–2581

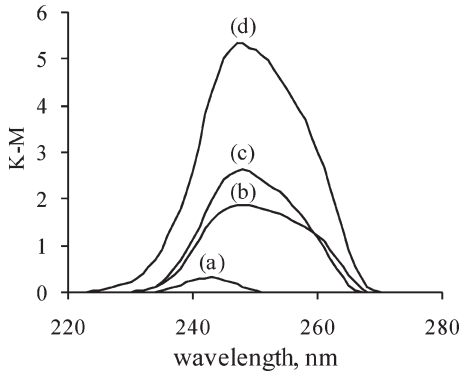

Figure 8. Diffuse reflectance UV−vis spectra of a 20 mM solution of $HgCl_2$ in $[C_4mim][NTf_2]$ in the absence (a) and presence of $[C_4mim]Cl$ (b, 40 mM; c, 80 mM; d, 120 mM).

species form in the solution,[24] which would then be reduced in a 2-electron step to Hg(0).

UV−Vis Studies. DR UV−vis spectra $HgCl_2$ in $[C_4mim][NTf_2]$ were carried out in the absence and presence of chloride (Figure 8). The spectrum of $HgCl_2$ shows a maximum at 242 nm, whereas the spectra of the solutions containing $[C_4mim]Cl$ all show a broad absorption peak with a maximum at 248 nm which increases in intensity as the concentration of Cl^- increases. The peaks have a shoulder at longer wavelength (ca. 260 nm), which is more accentuated in the solution with 40 mM of added Cl^-.

These results indicate that $HgCl_2$ reacts with the added Cl^- in the ionic liquid, in agreement with the voltammetric studies discussed above. The maximum at 248 nm is, therefore, assigned to $[HgCl_4]^{2-}$. A red shift in the absorption of $[HgCl_4]^{2-}$ with respect to that of $HgCl_2$ has also been reported in aqueous[25] and acetonitrile[26] solutions. In these solvents, the λ_{max} for $HgCl_2$ and $[HgCl_4]^{2-}$ appears at ca. 200 and 230 nm, respectively. The shoulder at 260 nm is tentatively assigned to $[HgCl_3]^-$, expected to be more abundant in the solution with the lowest amount of Cl^-. In acetonitrile, the absorption maximum of $[HgCl_3]^-$ (240 nm) is also observed at longer wavelength than that of $[HgCl_4]^{2-}$ (234 nm).[25]

CONCLUSIONS

The electrochemistry of Hg(II) in room temperature ionic liquids is strongly influenced by the nature of the working electrode (GC or Pt), the concentration of the solution, and the ionic liquid composition. In $HgCl_2/[C_4mim][NTf_2]$ solutions, a certain amount of Hg(II)−NTf_2^- and/or mixed-ligand Hg(II)−$[NTf_2]^-/Cl^-$ species form which are reduced to Hg(0) at a more positive potential than the main Hg(II) species present in the $HgCl_2$ solution, $[Hg^{2+}]_{Cl}$, as indicated by comparison with the CVs of $[Hg(NTf_2)_2]$ in $[C_4mim][NTf_2]$. At GC electrode, the reduction of $[Hg^{2+}]_{Cl}$ to Hg(0) occurs in one step, with similar behavior also observed for dilute solutions at Pt electrode. However, in concentrated solutions at Pt electrodes, the reduction of Hg(II) to Hg(0) takes place in three steps, related to the formation of intermediate species Hg_2^{2+} and Hg_3^{2+}. The reduction of Hg(II) in other $[NTf_2]^-$-based ionic liquids (dilute solutions) is qualitatively the same as that in $[C_4mim][NTf_2]$. Analogous behavior is also found in ionic liquids containing different anions. Shifting in the reduction potentials with IL composition is related mainly to the different viscosity of the media.

In the presence of an excess of a strongly complexing agent (i.e., in $[C_4mim][NTf_2]$ with added chloride or in $[C_4mim][DCA]$), anionic species of the type $[HgX_{2+x}]^{x-}$ (X = Cl, DCA) appear to be predominant in solution, and are reduced in a single 2-electron reduction to Hg(0). The scans for these systems depicted nucleation loops. Chronoamperometric studies on a 1:2 $HgCl_2$:Cl^- solution in $[C_4mim][NTf_2]$ at GC indicated that the nucleation of mercury takes place through an instantaneous process.

The reoxidation of Hg also showed unusual behavior with two to four peaks observed in the reverse scans (except in $[C_4mim][FAP]$). The first two peaks are related to the oxidation of Hg to Hg_2^{2+} and Hg^{2+}, whereas the peaks appearing at more positive potentials correspond to the oxidation of Cl^- attached to mercury. Results suggest that various chloromercurate(II) species form during the oxidative scans, including $[HgCl_3]^-$ and $[HgCl_4]^{2-}$, even in solutions with no added chloride.

ASSOCIATED CONTENT

Supporting Information. X-ray powder diffraction patterns; dimensionless plots generated from the nucleation profiles; cyclic voltammograms; and viscosities of the ionic liquids used in this work. This material is available free of charge via the Internet at http://pubs.acs.org.

AUTHOR INFORMATION

Corresponding Author

*E-mail: c.lagunas@qub.ac.uk (M.C.L.); c.hardacre@qub.ac.uk (C.H.).

ACKNOWLEDGMENT

Merck KGaA is thanked for its generous supply of ionic liquids. N.S.A.M. acknowledges the financial support of the Ministry of Higher Education Malaysia and University of Malaya via a SLAI fellowship.

REFERENCES

(1) Visser, A. E.; Swatloski, R. P.; Reichert, W. M.; Mayton, R.; Sheff, S.; Wierzbicki, A.; Davis, J. H.; Rogers, R. D. *Chem. Commun.* **2001**, 135–136. Visser, A. E.; Swatloski, R. P.; Reichert, W. M.; Mayton, R.; Sheff, S.; Wierzbicki, A.; Davis, J. H.; Rogers, R. D. *Environ. Sci. Technol.* **2002**, *36*, 2523–2529. Wei, G.; Yang, Z.; Chen, C. *Anal. Chim. Acta* **2003**, *488*, 183–192. Germani, R.; Mancini, M. V.; Savelli, G.; Spreti, N. *Tetrahedron Lett.* **2007**, *48*, 1767–1769. Ji, L.; Thiel, S. W.; Pinto, N. G. *Ind. Eng. Chem. Res.* **2008**, *47*, 8396–8400. Pena-Pereira, F.; Lavilla, I.; Bendicho, C.; Vidal, L.; Canals, A. *Talanta* **2009**, *78*, 537–541.

(2) Welton, T. *Chem. Rev.* **1999**, *99*, 2071–2083. Buzzeo, M. C.; Evans, R. G.; Compton, R. G. *ChemPhysChem* **2004**, *5*, 1106–1120. Buzzeo, M. C.; Hardacre, C.; Compton, R. G. *ChemPhysChem* **2006**, *7*, 176–180. Endres, F.; Zein El Abedin, S. *Phys. Chem. Chem. Phys.* **2006**, *8*, 2101–2116. Rogers, E. I.; Sljukic, B.; Hardacre, C.; Compton, R. G. *J. Chem. Eng. Data* **2009**, *54*, 2049–2053.

(3) Xu, X. H.; Hussey, C. L. *J. Electrochem. Soc.* **1993**, *140*, 1226–1233.

(4) Laitinen, H. A.; Liu, C. H.; Ferguson, W. S. *Anal. Chem.* **1958**, *30*, 1266–1270.

(5) Hanck, K. W.; Deanhardt, M. L. *Anal. Chem.* **1973**, *45*, 176–179.

(6) Deanhardt, M. L.; Hanck, K. W. *J. Electrochem. Soc.* **1976**, *123*, 1824–1827.

(7) Hames, D. A.; Plambeck, J. A. *Can. J. Chem.* **1968**, *46*, 1727–1733.

(8) Torsi, G.; Mamantov, G. *Inorg. Nucl. Chem. Lett.* **1970**, *6*, 843–846. Torsi, G.; Fung, K. W.; Begun, G. M.; Mamantov, G. *Inorg. Chem.* **1971**, *10*, 2285–2290.
(9) Chen, H.; He, Y.; Zhu, J.; Alias, H.; Ding, Y.; Nancarrow, P.; Hardacre, C.; Rooney, D.; Tan, C. *Int. J. Heat Fluid Flow* **2008**, *29*, 149–155.
(10) Cammarata, L.; Kazarian, S. G.; Salter, P. A.; Welton, T. *Phys. Chem. Chem. Phys.* **2001**, *3*, 5192–5200.
(11) Rogers, E. L.; Silvester, D. S.; Poole, D. L.; Aldous, L.; Hardacre, C.; Compton, R. G. *J. Phys. Chem. C* **2008**, *112*, 2729–2735.
(12) Singh, S.; DesMarteau, D. D. *Inorg. Chem.* **1986**, *25*, 4596–4597.
(13) Wang, Y.; Mo, J.; Cai, W.; Yao, L.; Zhang, L. *Chem. Lett.* **2001**, *30*, 434–435. Zhang, X.; Xie, Y.; Yu, W.; Zhao, Q.; Jiang, M.; Tian, Y. *Inorg. Chem.* **2003**, *42*, 3734–3737.
(14) Speranskaya, E. F.; Pokhvalitova, T. G. *Russ. Chem. Rev.* **1968**, *37*, 710–715. Jagner, D.; Sahlin, E.; Renman, L. *Anal. Chem.* **1996**, *68*, 1616–1622. Nolan, M. A.; Kounaves, S. P. *Anal. Chem.* **1999**, *71*, 1176–1182. Serruya, A.; Mostany, J.; Scharifker, B. R. *J. Electroanal. Chem.* **1999**, *464*, 39–47.
(15) Hine, F.; Yasuda, M.; Iwata, M. *J. Electrochem. Soc.* **1974**, *121*, 749–756. Bishop, E.; Cofre, P. *Analyst* **1981**, *106*, 433–438.
(16) Wang, J.; Lin, M. S. *Anal. Chem.* **1988**, *60*, 499–502.
(17) Aldous, L.; Silvester, D. S.; Villagran, C.; Pitner, W. R.; Compton, R. G.; Lagunas, M. C.; Hardacre, C. *New J. Chem.* **2006**, *30*, 1576–1583.
(18) Scharifker, B.; Hills, G. *Electrochim. Acta* **1983**, *28*, 879–889.
(19) Ilangovan, G.; Zweier, J. L.; Kuppusamy, P. *J. Phys. Chem. B* **2000**, *104*, 4047–4059. Bento, F. R.; Mascaro, L. H. *Surf. Coat. Technol.* **2006**, *201*, 1752–1756.
(20) Hyde, M. E.; Compton, R. G. *J. Electroanal. Chem.* **2003**, *549*, 1–12.
(21) Bauer, E.; Nowotny, H.; Stempfl, A. *Monatsh. Chem.* **1953**, *84*, 692–700. Ghosh, T.; Zhou, Q.; Gregoire, J. M.; Dover, R. B. v.; DiSalvo, F. J. *J. Phys. Chem. C* **2010**, *114*, 12545–12553.
(22) Robbins, G. D.; Enke, C. G. *J. Electroanal. Chem.* **1969**, *23*, 343–349.
(23) Endres, F.; Hofft, O.; Borisenko, N.; Gasparotto, L. H.; Prowald, A.; Al-Salman, R.; Carstens, T.; Atkin, R.; Bund, A.; El Abedin, S. Z. *Phys. Chem. Chem. Phys.* **2010**, *12*, 1724–1732.
(24) Köhler, H.; Nefedov, V. I.; Birkner, G.; Jeschke, M.; Kolbe, A. *Z. Anorg. Allg. Chem.* **1986**, *542*, 59–64. Köhler, H.; Skirl, R.; Jeschke, M. *Z. Chem.* **1984**, *24*, 444–445.
(25) Langmuir, M. E.; Hayon, E. *J. Phys. Chem.* **1967**, *71*, 3808–3814.
(26) Horvath, O.; Vogler, A. *Inorg. Chem.* **1993**, *32*, 5485–5489.